ZOOLOGICAL RESEARCH

A tree shrew model for steroid-associated osteonecrosis

DEAR EDITOR,

Osteonecrosis is a common human disease in orthopedics. It is difficult to treat, and half of patients may need artificial joint replacement, resulting in a considerable economic burden and a reduction in quality of life. Hormones are one of the major causes of osteonecrosis and high doses of corticosteroids are considered the most dangerous factor. Because of the complexity of treatment, we still need a better animal model that can be widely used in drug development and testing. Tree shrews are more closely related to primates than rodents. As such, we constructed a successful tree shrew model to establish and evaluate steroid-associated osteonecrosis (SAON). We found that low-dose lipopolysaccharide (LPS) combined with high-dose methylprednisolone (MPS) over 12 weeks could be used to establish a tree shrew model with femoral head necrosis. Serum biochemical and histological analyses showed that an ideal model was obtained. Thus, this work provides a useful animal model for the study of SAON and for the optimization of treatment methods.

SAON is a multifactorial disease, with high-dose corticosteroid administration thought to be the greatest risk factor (Amanatullah et al., 2011; Mont et al., 2006). SAON is a common refractory disease in the field of orthopedics, and its etiologies and non-operative and operative methods of treatment are complex (Wang et al., 2018). To improve preclinical research on SAON, an ideal disease animal model is urgently needed.

Animal models play key roles in identifying treatments for various types of disease, including SAON (Xu et al., 2018). In the present study, we developed a new animal model of steroid-induced femoral head necrosis using tree shrews (*Tupaia belangeri*, *Mammalia*, *Scandentia*, and *Tupaiidae*) found in the Yunnan region of China (Wang, 1987). Although rats, mice, rabbits, chickens, pigs, and emus have been used to establish various models of SAON (Beckmann et al., 2014; Bekler et al., 2007; Cui et al., 1997; Ryoo et al., 2014; Sun et al., 2011; Xi et al., 2017; Zheng et al., 2013), tree shrews are much more closely associated with primates in comparison at the behavioral, anatomical, genomic, and evolutionary levels (Bekler et al., 2007; Petruzziello et al., 2012; Xu et al., 2018; Zhang et al., 2013). Tree shrews have short reproductive and life cycles, high reproductivity, moderate size, and are easy to feed. They possess many features similar to those of humans and are frequently used as an experimental model in biomedical research (Xing et al., 2015; Yao, 2017; Ye et al., 2016). For example, tree shrews have been used in models of hepatitis virus infection, myopia, social stress, depression, metabolic diseases, and osteoporosis, and have shown many unique advantages (Wang et al., 2019; Xiao et al., 2017). With the development of genetic technology, the species will be increasingly used (Li et al., 2017; Yao, 2017). Whole-genome sequencing has revealed that tree shrews have a higher homology with humans than mice, rats, and dogs (Fan et al., 2013, 2019).

In this study, we used a low dose of LPS combined with a high dose of MPS to induce a model of femoral head necrosis in tree shrews. The model was established in 12 weeks as determined by biochemical analysis, micro-CT examinations, histological analyses, and scanning electron microscopy (SEM) (Supplementary Methods). A total of 12 healthy male tree shrews (six months old) were used in this study. All animal experiments were conducted in accordance with the guidelines created by the Kunming University Institutional Committee for the Care and Use of Laboratory Animals and were approved by the Kunming University Laboratory Animal Management Ethics Committee. Both the Guide for the Care and Use of Laboratory Animal (2011) (National Research Council Committee for the Update of the Guide for the Care and Use of Laboratory Animals, 2011) and the Animals in Research: Reporting *In Vivo* Experiments (ARRIVE) guidelines (Kilkenny et al., 2012) were followed.

Received: 24 April 2020; Accepted: 22 July 2020; Online: 29 July 2020

Foundation items: This study was supported by the National Science and Key Technology Support Program (2014BAI01B01-07) and Science and Technology Key Projects of Kunming (2014-04-A-S-01-3072)

DOI: 10.24272/j.issn.2095-8137.2020.061

To detect changes in blood biochemical indicators, the levels of bone alkaline phosphatase (BALP), bone GLA protein (BGP), N-terminal propeptide of type I collagen (P1NP), and C-terminal propeptide of type I collagen (P1CP) in serum samples from two tree shrew groups were determined using appropriate assay kits (Supplementary Figure S1). Results showed that the levels of BALP in the SAON group were significantly higher than those in the control group (P<0.001; Supplementary Figure S1A). Similarly, the levels of BGP, P1NP, and P1CP in the SAON group were significantly increased compared to those in the control group (P<0.05; Supplementary Figure S1B–D). These results indicated that there was a significant difference between the SAON and control groups in certain aspects of blood biochemical indicators, and the increases in bone metabolism markers reflected a high bone turnover rate in the SAON group.

Micro-CT examination showed that the shape of the femoral head had changed in the SAON group, with evidence of subchondral trabecular bone deterioration (Figure 1A). Bone mineral density (BMD), bone tissue volume fraction (BV/TV), and trabecular number (Tb. N) in the SAON group were all significantly lower than those in the control group (all P<0.05) (Table 1; Figure 1B), whereas trabecular separation (Tb. Sp) in the SAON group was significantly higher than that in the control group (P<0.05) (Table 1; Figure 1B). Mean trabecular thickness (Tb. Th) in the SAON group was lower than that in the control group, but the difference was not significant (P>0.05; Table 1; Figure 1B). In addition, the mean bone surface/volume ratio (BS/BV) in the SAON group was higher than that in the control group, but the difference was not significant (P>0.05; Table 1; Figure 1B).

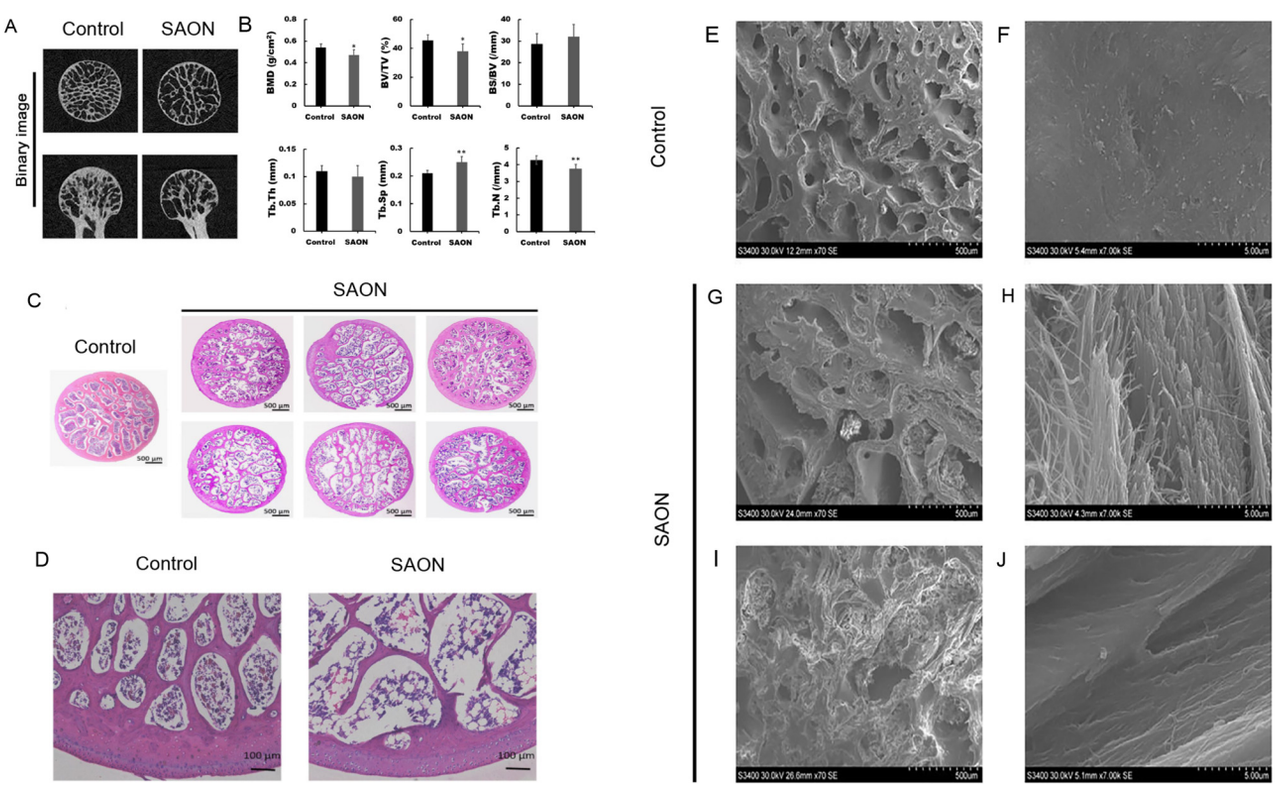

Figure 1 Micro-CT analysis, histological evaluation, and SEM analysis of femoral heads in control and SAON groups

A: In control group, femoral heads were properly shaped, with no evidence of cortical bone collapse, and trabecular bone was uniform, dense, continuous, and of normal thickness. In SAON group, femoral heads showed changes in shape, with evidence of cortical bone partial collapse, trabecular fracture, trabecular sparseness, thinning, and increased intercellular spacing. B: Micro-CT evaluation of control and SAON groups. All data are presented as mean±*SD* (n=6). *: P<0.05, **: P<0.01, vs. control group. BMD: Bone mineral density; BV/TV: Bone tissue volume fraction; BS/BV: Bone surface/volume ratio; Tb. N: Trabecular number; Tb. Th: Trabecular thickness; Tb. Sp: Trabecular separation. C, D: In control group, bone trabeculae were dense and intact, rich in bone marrow cells, and contained only a few fused adipose cells. In SAON group, trabecular bone displayed a disordered structure that appeared thinner and sparser, showed partial fractures, and contained adipose cells that were fused into vacuoles; bone trabeculae in SAON group contained more empty lacunae when compared to those in control group. E, F: In control group, bone trabeculae were dense, trabecular spacing was small (at low magnification), trabecular surface was smooth, and there were dense bone fibers (at high magnification). G–J: In SAON group, bone trabeculae were sparser, trabecular spacing was increased (at low magnification), and trabecular bone surface was disordered (at high magnification).

Table 1 Micro-CT evaluation of control and SAON groups (*n*=6, X±S)

Group	BMD value	BV/TV (%)	BS/BV (/mm)	Tb. Th (mm)	Tb. Sp (mm)	Tb. N (/mm)
Control	0.541 0±0.033 3	45.43±3.87	28.72±4.69	0.11±0.01	0.21±0.01	4.28±0.22
SAON	0.470 9±0.049 2*	38.03±5.05*	32.11±5.53△	0.10±0.02△	0.25±0.02**	3.77±0.27**

BMD: Bone mineral density; BV/TV: Bone tissue volume fraction; BS/BV: Bone surface/volume ratio; Tb. Th: Trabecular thickness; Tb. Sp: Trabecular separation; Tb. N: Trabecular number. Compared with control group, △: $P>0.05$, *: $P<0.05$, **: $P<0.01$.

Examination of tissue sections showed that in the control group, the bone trabeculae were dense, intact, rich in bone marrow cells, and contained only a few adipose cells. In contrast, the trabecular bone in the SAON group appeared to be thinner and sparser, somewhat fractured, and displayed a disordered cellular structure; furthermore, the adipose cells were fused into vacuoles (Figure 1C). In addition, there were more empty lacunae in the SAON group than in the control group (Figure 1D). SEM also showed that in the control group, the bone trabeculae were dense, trabecular spacing was small (at low magnification, Figure 1E), trabecular surface was smooth, and bone fibers showed a dense appearance (at high magnification, Figure 1F). In the SAON group, the trabeculae were much sparser, trabecular spacing was increased (at low magnification, Figure 1G, I), and the trabecular bone surface was disordered (at high magnification, Figure 1H, J).

TUNEL staining results showed that in the control group, there were more cells in each tissue section, but fewer cells were stained green (Supplementary Figure S2A). In the SAON group, there were fewer cells in each section, but more cells were stained green (Supplementary Figure S2B). These findings suggest that more cells in the SAON group were undergoing apoptosis.

Our study employed a combined pulsed LPS and MPS induction protocol previously used for measuring steroid-induced femoral head necrosis in numerous animal models (Qin et al., 2006; Zheng et al., 2013, 2018). This induction protocol has been successfully applied to establish a rabbit model of SAON and involved a single injection of low-dose (10 μg/kg) LPS, followed by three injections of high-dose (20 mg/kg) MPS, resulting in a high incidence SAON but low rate of mortality in the treated rabbits (Qin et al., 2006). SAON has also been successfully induced in Sprague-Dawley rats by an intravenous injection of LPS (0.2 mg/kg), followed by three intraperitoneal injections of MPS (100 mg/kg) over a 24 h interval, and further intraperitoneal injections of MPS (40 mg/kg) three times per week for six weeks (Zheng et al., 2018). An emu SAON model was successfully established after 24 weeks using two intravenous injections of LPS (8 mg/kg body weight) via the jugular vein, followed by three intramuscular injections (10 mg/kg body weight into the gluteus muscle) at an interval of two days (Zheng et al., 2013). In this study, we induced SAON in tree shrews by giving one intravenous injection of LPS (300 μg/kg), followed by three intraperitoneal injections of MPS (130 mg/kg) over a 24 h interval; after which, MPS (130 mg/kg) was intraperitoneally injected two times per week for 12 weeks. The dosages and induction times of LPS and MPS are different from those used for other animals.

As biochemical markers of bone formation, BALP, BGP, P1NP, and P1CP can be used to detect osteoporosis and femoral head necrosis (Mohamed et al., 2014). BGP is secreted by bone cells (Cantatore et al., 1991), osteoblasts, and osteoclasts (Quan et al., 2012), BALP is a specific and sensitive biochemical indicator of bone metabolism, whereas P1NP and P1CP reflect osteoblast activity and bone formation. While these indicators all exist in normal blood, their levels are elevated in osteoporotic and osteoarthritic patients (Garnero et al., 1996; Szulc & Delmas, 2008). The elevated levels of these bone formation markers in our study may be due to viable osteoblasts attempting to replenish lost bone tissue (Chan et al., 2006).

As described previously, femoral head necrosis is a type of systemic skeletal disease characterized by bone loss and degradation of bone tissue microstructure, accompanied by increased bone fragility and fracture susceptibility (De Ruijter et al., 2013). It is widely accepted that BMD in the proximal femur decreases after osteonecrosis occurs (Fazzalari et al., 2002). The bone loss that occurs in the proximal femur after osteonecrosis in a remodeled femoral head results from stress shielding due to stiffness of the implant caused by bone during growth (Calder et al., 2001). Our results showed that BMD of the right femoral heads in the SAON group decreased significantly compared with that in the control group. Furthermore, examination of bone microarchitecture in the SAON group revealed rarefaction and fracture of trabecular bone due to decreased cortical bone thickness and trabecular bone area. These results suggest that bone quality was significantly lower in the SAON group.

Histological and micro-electron microscopy analyses of the femoral heads were performed, especially in the central portions of the femoral heads (Kim & Kim, 2004). Micro-CT evaluations of the femoral heads, where bone structure collapse was demonstrated, indicated that the pulsed LPS-MPS induction protocol produced femoral head necrosis, as differences in bone structure and BMD were found between the SAON and control groups in regions that were distant from the subchondral bone. This finding is similar to that reported in another bone densitometry study conducted in a steroid-induced osteonecrosis model (Janke et al., 2013).

In short, we successfully replicated a tree shrew model of human hormone-induced osteonecrosis. Thus, this work provides a useful animal model for the study of SAON and optimization of treatment methods.

SUPPLEMENTARY DATA

Supplementary data to this article can be found online.

COMPETING INTERESTS

The authors declare that they have no competing interests.

AUTHORS' CONTRIBUTIONS

Z.X.M., M.H., and Y.J.L. conceived and designed the study. B.L.L., T.K.M., P.F.B., X.F.W., C.T.Y., and D.P.M. performed the experiments. Q.C., Z.X.M., H.S., and W.L.W. wrote the initial manuscript. Z.N.Y., L.B.X., Y.Y.H., and W.G.W. were responsible for data and statistical analyses. D.X.K. and J.J.D. reviewed the findings and R.P.Z. checked the acquired data, helped to analyze and interpret the data, and edited the manuscript. All authors read and approved the final version of the manuscript.

Qi Chen[1,#], Zhao-Xia Ma[2,#], Li-Bin Xia[3,#], Zhen-Ni Ye[3], Bao-Ling Liu[4], Tie-Kun Ma[4], Peng-Fei Bao[2], Xing-Fei Wu[2], Cong-Tao Yu[2], Dai-Ping Ma[2], Yuan-Yuan Han[5], Wen-Guang Wang[5], De-Xuan Kuang[5], Jie-Jie Dai[5], Rong-Ping Zhang[6], Min Hu[2], Hong Shi[1,*], Wen-Lin Wang[7,*], Yan-Jiao Li[2,*]

[1] *Yunnan Key Laboratory of Primate Biomedical Research*, *Institute of Primate Translational Medicine*, *Kunming University of Science and Technology*, *Kunming*, *Yunnan* 650500, *China*
[2] *Yunnan Key Laboratory for Basic Research on Bone and Joint Diseases* & *Yunnan Stem Cell Translational Research Center*, *Kunming University*, *Kunming*, *Yunnan* 650214, *China*
[3] *Department Obstetrics*, *Second Affiliated Hospital of Kunming Medical University*, *Kunming*, *Yunnan* 650101, *China*
[4] *Department of Nuclear Medicine*, *First Affiliated Hospital of Kunming Medical University*, *Kunming*, *Yunnan* 650031, *China*
[5] *Center of Tree Shrew Germplasm Resources*, *Institute of Medical Biology*, *Chinese Academy of Medical Sciences and Peking Union Medical College*, *Kunming*, *Yunnan* 650118, *China*
[6] *School of Chinese Materia Medica*, *Yunnan University of Chinese Medicine*, *Kunming*, *Yunnan* 650500, *China*
[7] *Kunming Medical University*, *Kunming*, *Yunnan* 650500, *China*
[#]Authors contributed equally to this work
*Corresponding authors, E-mail: shih@kust.edu.cn; wenlinwang331@163.com; 391910123@qq.com

REFERENCES

Amanatullah DF, Strauss EJ, Di Cesare PE. 2011. Current management options for osteonecrosis of the femoral head: part II, operative management. *American Journal of Orthopedics*, **40**(10): E216−E225.

Beckmann R, Shaheen H, Kweider N, Ghassemi A, Fragoulis A, Hermanns-Sachweh B, et al. 2014. Enoxaparin prevents steroid-related avascular necrosis of the femoral head. *The Scientific World Journal*, **2014**: 347813.

Bekler H, Uygur AM, Gökçe A, Beyzadeoğlu T. 2007. The effect of steroid use on the pathogenesis of avascular necrosis of the femoral head: an animal model. *Acta Orthopaedica et Traumatologica Turcica*, **41**(1): 58−63.

Calder JDF, Pearse MF, Revell PA. 2001. The extent of osteocyte death in the proximal femur of patients with osteonecrosis of the femoral head. *The Journal of Bone and Joint Surgery*, **83–B**(3): 419−422.

Cantatore FP, Carrozzo M, Magli DM, Pipitone V. 1991. Mononuclear cells are not involved in BGP synthesis and secretion. *Clinical Rheumatology*, **10**(1): 28−30.

Chan MHM, Chan PKS, Griffith JF, Chan IHS, Lit LCW, Wong CK, et al. 2006. Steroid-induced osteonecrosis in severe acute respiratory syndrome: a retrospective analysis of biochemical markers of bone metabolism and corticosteroid therapy. *Pathology*, **38**(3): 229−235.

Cui QJ, Wang GJ, Su CC, Balian G. 1997. The Otto Aufranc Award. Lovastatin prevents steroid induced adipogenesis and osteonecrosis. *Clinical Orthopaedics and Related Research*, (344): 8−19.

De Ruijter J, Maas M, Janssen A, Wijburg FA. 2013. High prevalence of femoral head necrosis in Mucopolysaccharidosis type III (Sanfilippo disease): a national, observational, cross-sectional study. *Molecular Genetics and Metabolism*, **109**(1): 49−53.

Fan Y, Huang ZY, Cao CC, Chen CS, Chen YX, Fan DD, et al. 2013. Genome of the Chinese tree shrew. *Nature Communications*, **4**: 1426−1426.

Fan Y, Ye MS, Zhang JY, Xu L, Yu DD, Gu TL, et al. 2019. Chromosomal level assembly and population sequencing of the Chinese tree shrew genome. *Zoological Research*, **40**(6): 506−521.

Fazzalari NL, Kuliwaba JS, Forwood MR. 2002. Cancellous bone microdamage in the proximal femur: influence of age and osteoarthritis on damage morphology and regional distribution. *Bone*, **31**(6): 697−702.

Garnero P, Hausherr E, Chapuy MC, Marcelli C, Grandjean H, Muller C, et al. 1996. Markers of bone resorption predict hip fracture in elderly women: the EPIDOS prospective study. *Journal of Bone and Mineral Research*, **11**(10): 1531−1538.

Janke LJ, Liu CC, Vogel P, Kawedia J, Boyd KL, Funk AJ, et al. 2013. Primary epiphyseal arteriopathy in a mouse model of steroid-induced osteonecrosis. *The American Journal of Pathology*, **183**(1): 19−25.

Kilkenny C, Browne WJ, Cuthill IC, Emerson M, Altman DG. 2012. Improving bioscience research reporting: the ARRIVE guidelines for reporting animal research. *Osteoarthritis and Cartilage*, **20**(4): 256−260.

Kim YH, Kim JS. 2004. Histologic analysis of acetabular and proximal femoral bone in patients with osteonecrosis of the femoral head. *The Journal of Bone and Joint Surgery*, **86**(11): 2471−2474.

Li CH, Yan LZ, Ban WZ, Tu Q, Wu T, Wang L, et al. 2017. Long-term propagation of tree shrew spermatogonial stem cells in culture and successful generation of transgenic offspring. *Cell Research*, **27**(2): 241−252.

Mohamed Y, Haifa H, Datel O, Fadoua HN, Smeh BH, Mahbouba J, et al. 2014. The role of biochemical markers of bone turnover in the diagnosis of osteoporosis and predicting fracture risk. *La Tunisie Medicale*, **92**(5): 304−310.

Mont MA, Jones LC, Hungerford DS. 2006. Nontraumatic osteonecrosis of the femoral head: ten years later. *The Journal of Bone & Joint Surgery*, **88**(5): 1117−1132.

National Research Council Committee for the Update of the Guide for The C & Use of Laboratory A. 2011. Guide for the Care and Use of Laboratory Animals. 8th ed. Washington, DC: National Academies Press.

Petruzziello F, Fouillen L, Wadensten H, Kretz R, Andren PE, Rainer G, et al. 2012. Extensive characterization of *Tupaia belangeri* neuropeptidome

using an integrated mass spectrometric approach. *Journal of Proteome Research*, **11**(2): 886−896.

Qin L, Zhang G, Sheng H, Yeung KW, Yeung HY, Chan CW, et al. 2006. Multiple bioimaging modalities in evaluation of an experimental osteonecrosis induced by a combination of lipopolysaccharide and methylprednisolone. *Bone*, **39**(4): 863−871.

Quan JJ, Zhou CX, Johnson NW, Francis G, Dahlstrom JE, Gao J. 2012. Molecular pathways involved in crosstalk between cancer cells, osteoblasts and osteoclasts in the invasion of bone by oral squamous cell carcinoma. *Pathology*, **44**(3): 221−227.

Ryoo S, Lee S, Jo S, Lee S, Kwak A, Kim E, et al. 2014. Effect of lipopolysaccharide (LPS) on mouse model of steroid-induced avascular necrosis in the femoral head (ANFH). *Journal of Microbiology and Biotechnology*, **24**(3): 394−400.

Sun Y, Feng Y, Zhang CQ, Cheng XG, Chen SB, Ai ZS, et al. 2011. Beneficial effect of autologous transplantation of endothelial progenitor cells on steroid-induced femoral head osteonecrosis in rabbits. *Cell Transplantation*, **20**(2): 233−243.

Szulc P, Delmas PD. 2008. Biochemical markers of bone turnover: potential use in the investigation and management of postmenopausal osteoporosis. *Osteoporosis International*, **19**(12): 1683−1704.

Wang A, Ren M, Wang JC. 2018. The pathogenesis of steroid-induced osteonecrosis of the femoral head: a systematic review of the literature. *Gene*, **671**: 103−109.

Wang YL, Ma ZX, Zheng YY, Liu BL, Bao PF, Wu XF, et al. 2019. Establishment of an osteoporosis model in tree shrews by bilateral ovariectomy and comprehensive evaluation. *Experimental and Therapeutic Medicine*, **17**(5): 3644−3654.

Wang YX. 1987. Taxonomic research on Burma-Chinese tree Shrew, Tupaia belangeri (Wagner), from Southern China. *Zoological Research*, **8**(3): 213−230. (in Chinese)

Xi HB, Tao WJ, Jian ZG, Sun XF, Gong XH, Huang LX, et al. 2017. Levodopa attenuates cellular apoptosis in steroid-associated necrosis of the femoral head. *Experimental and Therapeutic Medicine*, **13**(1): 69−74.

Xiao J, Liu R, Chen CS. 2017. Tree shrew (*Tupaia belangeri*) as a novel laboratory disease animal model. *Zoological Research*, **38**(3): 127−137.

Xing HJ, Jia K, He J, Shi CZ, Fang MX, Song LL, et al. 2015. Establishment of the tree shrew as an alcohol-induced Fatty liver model for the study of alcoholic liver diseases. *PLoS One*, **10**(6): e0128253.

Xu JZ, Gong HP, Lu ST, Deasey MJ, Cui QJ. 2018. Animal models of steroid-induced osteonecrosis of the femoral head —a comprehensive research review up to 2018. *International Orthopaedics*, **42**(7): 1729−1737.

Yao YG. 2017. Creating animal models, why not use the Chinese tree shrew (*Tupaia belangeri chinensis*)?. *Zoological Research*, **38**(3): 118−126.

Ye LH, He M, Huang YC, Zhao GQ, Lei YJ, Zhou YC, et al. 2016. Tree shrew as a new animal model for the study of lung cancer. *Oncology Letters*, **11**(3): 2091−2095.

Zhang XH, Dai ZX, Zhang GH, Han JB, Zheng YT. 2013. Molecular characterization, balancing selection, and genomic organization of the tree shrew (*Tupaia belangeri*) MHC class I gene. *Gene*, **522**(2): 147−155.

Zheng LZ, Liu Z, Lei M, Peng J, He YX, Xie XH, et al. 2013. Steroid-associated hip joint collapse in bipedal emus. *PLoS One*, **8**(10): e76797.

Zheng LZ, Wang JL, Kong L, Huang L, Tian L, Pang QQ, et al. 2018. Steroid-associated osteonecrosis animal model in rats. *Journal of Orthopaedic Translation*, **13**: 13−24.